Supplementary Material for "Time-scaling in Atomistics and the Rate-Dependent Mechanical Behavior of Nanostructures"

Xin Yan[1] and Pradeep Sharma[1,2,3,*]
[1] *Department of Mechanical Engineering, University of Houston, Houston, Texas, 77004 USA*
[2] *Department of Physics, University of Houston, Houston, Texas, 77004 USA*
[3] *Material Science and Engineering Program, University of Houston, Houston, Texas, 77004 USA*
[*] *Email: psharma@uh.edu. Phone: +1 713-7434502*

I. IMPLEMENTATION OF STRAIN RATE

We implement a constant strain rate ($\dot{\varepsilon}$) in the following way (as shown in the flowchart in Fig. S1 below). Under a given strain, the current potential energy surface (PES) is sampled by ABC and multiple energy minima are identified. Then Nudged Elastic Band (NEB) is used to calculate accurate barriers from the initial well to all the possible final states identified in the ABC sampling. Kinetic Monte Carlo (KMC) is used to select a transition path and harmonic Transition State Theory (h-TST) is used to calculate the transition time between the initial and selected final states (more simulation details can be found in Section III). Finally, the transition time multiplied by defined strain rate ($\dot{\boldsymbol{\varepsilon}}$) yields the strain increment for the next iteration through

$$\Delta\boldsymbol{\varepsilon} = \dot{\boldsymbol{\varepsilon}}\Delta t \tag{1}$$

where Δt is transition time in each increment and it is calculated from h-TST. Then, the strain increment is applied to the system and a new round of ABC sampling (and the entire aforementioned process) is repeated.

We calculate the total time from the total deformation (strain $\boldsymbol{\varepsilon}$) and the constant strain rate ($\dot{\boldsymbol{\varepsilon}}$) we have defined through the relation $t = \boldsymbol{\varepsilon}/\dot{\boldsymbol{\varepsilon}}$. This should provide a fairly tight control over the transition time between minima if the strain increments are "small enough". In this work, to assure this, indeed such small increments (for example $\Delta\boldsymbol{\varepsilon} < 5 \times 10^{-3}$) were applied to the system during each iteration (strain increment).

II. COMPARISON OF OUR APPROACH WITH OTHER ABC-BASED METHODS

In ABC sampling, due to the manner in which the penalties are applied, the system never comes back to energy well it has visited. In this way, the original ABC approach[1, 2] ignores the appearance of other possible jumps from the current state and may lead a significant overestimation of time. The algorithm in Ref. [3] improves upon this situation in the context of *strain-rate controlled tests*. In turn, we have also made a further (arguably minor) improvement to the algorithm reported in [3] designed to apply a constant strain rate to the system. In reference [3], for every PES sampling, ABC stopped as long as a new energy state is identified. In our work, we continue ABC sampling until multiple minima are identified. Then we calculate barriers from the initial minimum to all the minima identified in ABC using NEB.

The time overestimation problem of original ABC may be fixed by extending the sampling-dimension i.e. by using the so-called extended-ABC approach referred to as ABC-E [4] (or other related methods like the dimer approach[5]). In this algorithm, after a new minimum is identified using ABC-sampling, a penalty is added on the saddle point to block the identified path. The system then is sent back to the initial state to find other possible minima around the initial state. The way ABC-E is adopted to search multiple transition paths is quite similar to Activation Relaxation Technique (ART) [6] and the dimer approach[5]. However, ABC-E approach is computationally quite heavy. The original ABC-based time-scaling approach is a depth-first sampling algorithm which only yields a single transition path and ignore all the others. This is to be distinguished from breadth-first scanning algorithms (such as ABC-E) which identify multiple possible transitions.

To make the arguments clear, in Table S1, we compare the original ABC based time-scaling approach [1, 7, 8], ABC-E [4] and the approach used in our work (modified from ref. [3]–we call it strain-rate controlled ABC). We hope

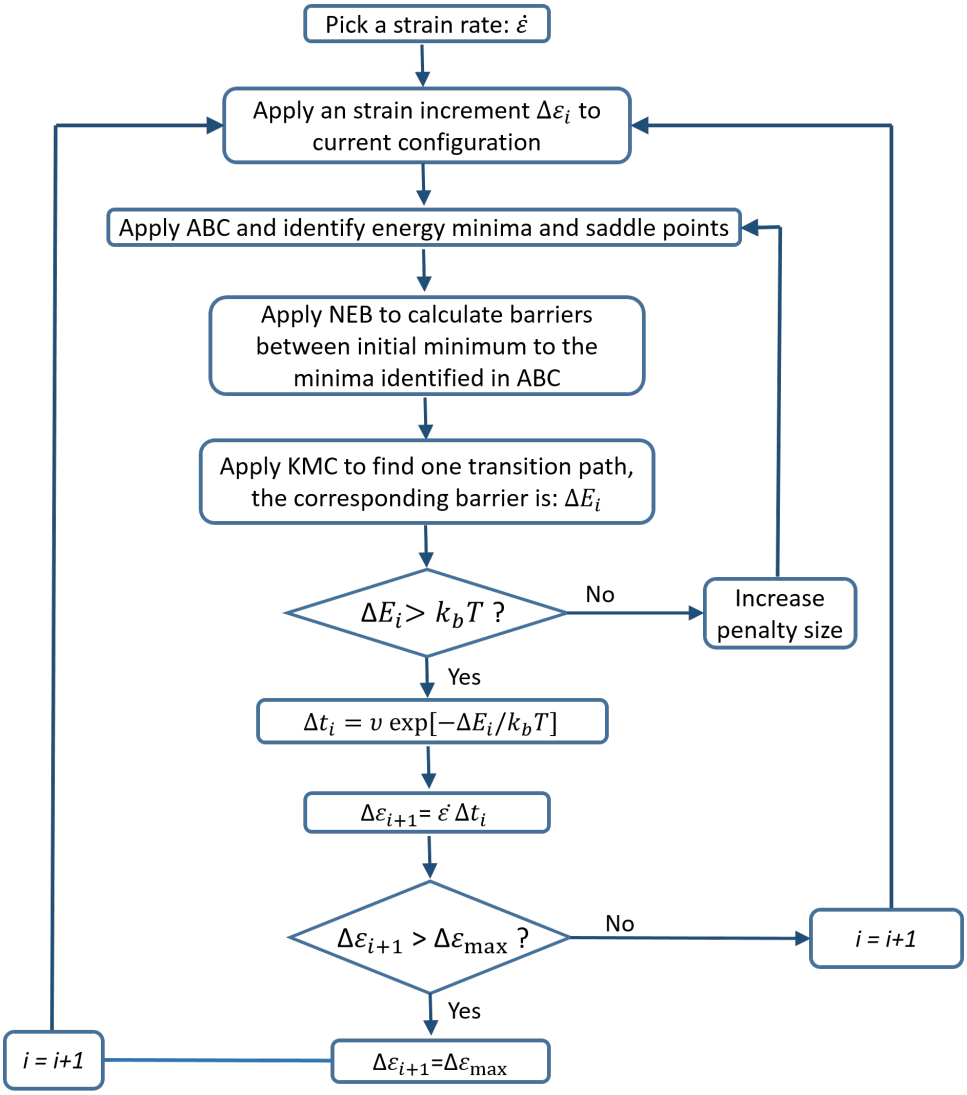

Figure S1. Imposition of strain rate in our approach.

that the material below is able to clearly delineate the differences among the various "ABCish" approaches.

III. SIMULATION DETAILS

We have implemented a parallel version of ABC algorithm in the LAMMPS[9]. For each ABC sampling, 100 penalties are added to the system. Usually, 5-10 minima are found for each small strain increment. We assume all the minima found in ABC are the possible final states in the current PES. NEB with 12 replica is adopted to find the barriers between initial minimum and all the possible final states identified in ABC. The convergence criteria for NEB is 1e-8 eV for energy and 1e-6 eV/Angstrom for force. With the barrier energies in hand, we use the harmonic transition state theory to estimate the rate constant for each event (barrier-crossing):

$$k_i \propto exp[-\Delta E / k_b T] \tag{2}$$

where k_i is the rate constant for the single jump from an initial minimum to a possible final minimum, ΔE is the barrier energy calculated from NEB, k_b is Boltzmann constant and T is temperature (300K). The rate constant of the single jump divided by the summation of all the rate constants calculated in the current PES, yields the probability

Table S1. Comparison of "ABCish "approaches

	Original ABC	ABC-E	Strain-rate controlled ABC
Simple description	Starting from current energy minimum, penalties are added to push the system to climb out of current energy well.	After a new minimum is identified using ABC, a penalty is added on the saddle point to block the identified path. The system then is set back to the initial state to find other possible minimum around the same initial state.	A constant strain rate is picked before simulation. The strain is applied in discrete steps and potential energy surfaces (PES') corresponding to each strain are sampled using ABC. Total time is calculated from the total deformation (strain $\boldsymbol{\varepsilon}$) and the constant strain rate ($\dot{\boldsymbol{\varepsilon}}$) through the relation $t = \boldsymbol{\varepsilon}/\dot{\boldsymbol{\varepsilon}}$.
Sampling dimension	Depth-first search	Breadth-first search	Multiple PES' are described
NEB is used to tighten the estimates of the barriers	Yes	Yes	Yes
KMC is used	Yes	Yes	Yes
Rate control	No	No	Yes
Control over time	Poor estimation of time	Acceptable	Acceptable if $\Delta\boldsymbol{\varepsilon}$ is small

of this single jump. One of the possible transition is randomly chosen based on the relative probabilities [10].

The PES evolves with the strain—i.e. with each increment of the strain. At each increment, we have to choose a different penalty size in ABC sampling. For every iteration, due to the constraint of maximum strain increment, a maximum time variation ($\Delta t_{max} = \Delta\boldsymbol{\varepsilon}_{max}/\dot{\boldsymbol{\varepsilon}}$) can be calculated. The maximum time is related to maximum barriers by $\Delta t_{max} = 10^{13} exp[-\Delta E_{max}/k_b T]$). In this way, we can estimate the upper limit to the energy barriers. In ABC sampling, we are only interested in rare events and therefore we ignore barriers smaller than the thermal fluctuation energy (0.0258 eV for 300K). In our simulations, the meaningful barrier ranges are 0.0258–0.119 eV for the high strain rate case and 0.0258–0.91 eV for the low strain rate case. The identified barriers are closely monitored during the simulations. If the barriers go out of the range, the simulation is terminated and the penalty size is adjusted to make sure the barriers identified are located in the range.

We use the nominal stress definition in all the plotted stress-strain curves. We use $\boldsymbol{\varepsilon} = dL/L$ to define the strain. The reference lengths for the small (112 atoms) and large (420 atoms) nano-slabs are 35.2Å and 70.4Å respectively.

IV. COMPUTATIONAL COST EVALUATION

In our work, the strain is applied to the system in discrete steps and the strain rate is a constant defined at the beginning of the simulation. Thus the computational cost depends on two factors: (i) the cost for ABC sampling during the iteration, NEB during the iteration, and KMC during the iteration and (ii) the number of strain increment (iteration) applied during loading. The summary of computational cost can be found in TABLE S2.

Table S2. Computational cost evaluation

	Small model with 116 atoms		Large model with 420 atoms	
ABC	2 minutes (1 processor)		8 minutes (2 processors)	
NEB	around 6 minutes (12 processors)		around 10 minutes (12 processors)	
Total time for single PES	around 9 minutes		around 20 minutes	
Number of strain increment	low strain rate	high strain rate	low strain rate	high strain rate
	559	1592	347	1860
Total time	4 day	10 day	5 day	25 day

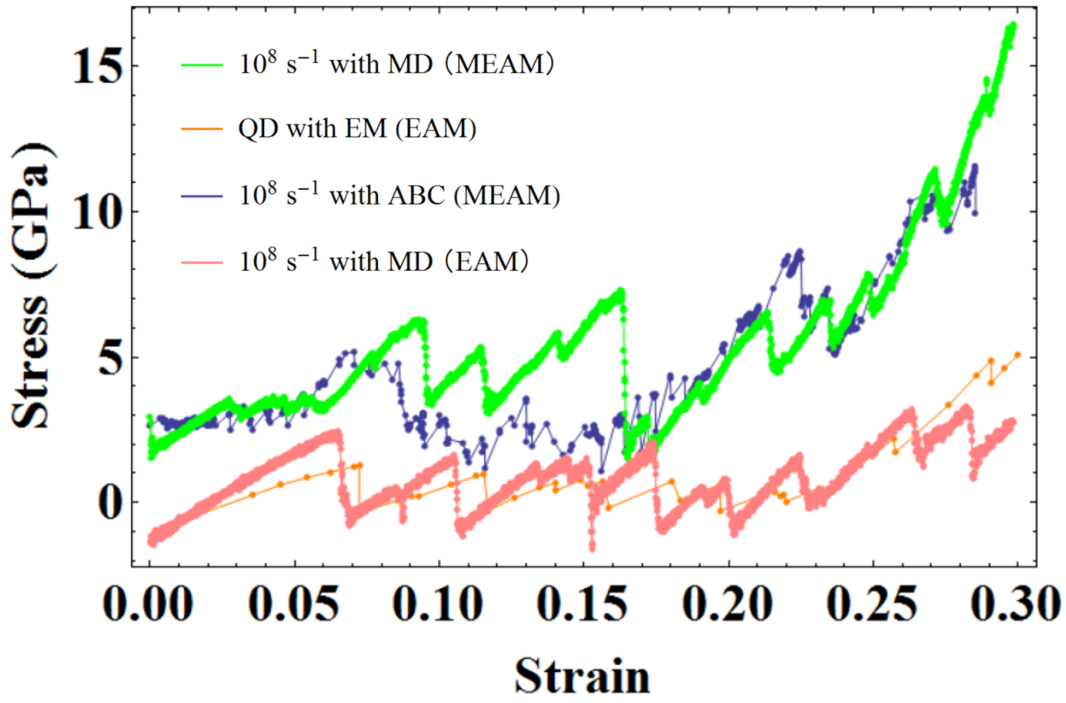

Figure S2. Comparison of stress-strain curves. Blue curve is strain-rate controlled ABC result of $10^8 s^{-1}$ case with MEAM potential; green curve is MD result of $10^8 s^{-1}$ case with MEAM potential; orange curve is QD process of equilibrium mapping (EM) method from Ref.[13] using EAM potential[11, 12]; pink curve is MD result of $10^8 s^{-1}$ case with EAM potential[11, 12].

KMC is very fast in the present context (less than 1 second) and accordingly we have excluded it from the table. The time shown in TABLE S2 is an approximation since for different strain increments, the lapsed time for each ingredient is slightly different. Unfortunately, the time in our actual calculations is different than what is reflected in the table. The reason is that the PES varies (or evolves) with each strain increment. Thus, in order to sample efficiently, we need to manually adjust the penalty parameters every few strain increments. This requires additional time and labor.

V. MOLECULAR DYNAMICS (MD) SIMULATIONS WITH DIFFERENT POTENTIALS

Molecular dynamics simulations of high strain rate ($10^8 s^{-1}$) compression with MEAM (green curve) and EAM (pink curve) [11, 12] potentials are shown in Fig.S2. We find that the MEAM based results matches our high-strain rate ABC calculation while the EAM based results match the QD evolution based on the PET approach[13]. Thus, we believe that the discrepancy of our stress curve and the one in Ref. [13] is due to the adoption of different potentials. The reason we adopted MEAM potential is because we expected the possibility of surface reconstructions and MEAM was precisely developed (as an extension of EAM) to better handle surface properties of metals.

VI. VIDEOS OF THE RESULTS

The following are the videos that illustrate the results. Please find attached AVI file named Video_S1, Video_S2, Video_S3, Video_S4, Video_S5 and Video_S6, Color coding of all the videos is same as Fig. 3a in main text.

1. Video S1 shows the deformation of the Ni nano-slab under compression at high strain rate (10^8 s^{-1}) using our approach;

2. Video S2 shows the deformation of the Ni nano-slab under compression at low strain rate (1 s^{-1}) using our approach;

3. Video S3 shows the deformation of the Ni nano-slab under compression at high strain rate ($10^8\ s^{-1}$) using conventional MD;

4. Video S4 shows the deformation of the large Ni nano-slab under compression at high strain rate ($10^8\ s^{-1}$) using our approach;

5. Video S5 shows the deformation of the large Ni nano-slab under compression at low strain rate ($1\ s^{-1}$) using our approach;

6. Video S6 shows the deformation of the large Ni nano-slab under compression at high strain rate ($10^8\ s^{-1}$) using conventional MD;

[1] Y. Fan, A. Kushima, S. Yip, and B. Yildiz, Physical review letters **106**, 125501 (2011).
[2] P. Brommer and N. Mousseau, Physical review letters **108**, 219601 (2012).
[3] Y. Fan, Y. N. Osetskiy, S. Yip, and B. Yildiz, Proceedings of the National Academy of Sciences **110**, 17756 (2013).
[4] Y. Fan, S. Yip, and B. Yildiz, Journal of Physics: Condensed Matter **26**, 365402 (2014).
[5] G. Henkelman and H. Jónsson, The Journal of chemical physics **111**, 7010 (1999).
[6] G. Barkema and N. Mousseau, Physical review letters **77**, 4358 (1996).
[7] A. Kushima, X. Lin, J. Li, J. Eapen, J. C. Mauro, X. Qian, P. Diep, and S. Yip, The Journal of chemical physics **130**, 224504 (2009).
[8] A. Kushima, J. Eapen, J. Li, S. Yip, and T. Zhu, The European Physical Journal B **82**, 271 (2011).
[9] S. Plimpton, Journal of computational physics **117**, 1 (1995).
[10] A. F. Voter, in *Radiation Effects in Solids* (Springer, 2007), pp. 1–23.
[11] J. E. Angelo, N. R. Moody, and M. I. Baskes, Modelling and Simulation in Materials Science and Engineering **3**, 289 (1995).
[12] M. Baskes, X. Sha, J. Angelo, and N. Moody, Modelling and Simulation in Materials Science and Engineering **5**, 651 (1997).
[13] S. Pattamatta, R. S. Elliott, and E. B. Tadmor, Proceedings of the National Academy of Sciences **111**, E1678 (2014).